

## STRANGE CEPHEIDS AND RR LYRAE

J. ROBERT BUCHLER<sup>1</sup>, ZOLTÁN KOLLÁTH<sup>2</sup>

ASTROPHYSICAL JOURNAL, to be submitted

### ABSTRACT

Strange modes can occur in radiative classical Cepheids and RR Lyrae models. These are vibrational modes that are trapped near the surface as a result of a 'potential barrier' caused by the sharp hydrogen partial ionization region. Typically the modal number of the strange mode falls between the 7th and 12th overtone, depending on the astrophysical parameters of the equilibrium stellar models (L, M,  $T_{\text{eff}}$ , X, Z). Interestingly these modes can be *linearly unstable outside the usual instability strip*, in which case they should be observable as new kinds of variable stars, 'strange Cepheids' or 'strange RR Lyrae' stars. The present paper reexamines the linear stability properties of the strange modes by taking into account the effects of an isothermal atmosphere, and of turbulent convection. It is found that the linear vibrational instability of the strange modes is resistant to both of these effects. Nonlinear hydrodynamic calculations indicate that the pulsation amplitude of these modes is likely to saturate at the millimagnitude level. These modes should therefore be detectable albeit not without effort.

*Subject headings:* oscillations of stars - Cepheids - s-Cepheids

<sup>1</sup>Physics Department, University of Florida, Gainesville, FL, USA

<sup>2</sup>Konkoly Observatory, Budapest, HUNGARY

### 1. INTRODUCTION

Strange modes were discovered and named by Saio, Wheeler & Cox (198) in highly nonadiabatic stars. (For a general reference *cf.* Gautschy & Saio 1996). In a recent paper (Buchler, Yecko & Kolláth 1997; hereafter Paper I) it was demonstrated that strange, or surface modes not only exist also in classical Cepheids, thrive there. Paper I showed that the strange modes are vibrational modes that are predominantly surface modes that exist quite naturally even in the adiabatic limit.

This was exhibited with the help of simple transformations of the radial coordinate to an acoustic depth  $z$ , defined through  $dz = dr/c_s$  and of the radial displacement vector  $\psi = \sqrt{\rho c_s} r \delta r$ , where  $c_s$  is the sound speed, with which the *adiabatic* radial pulsation problem for radiative models can be reduced to a time-independent Schrödinger equation

$$-\frac{d^2\psi}{dz^2} + V(z)\psi = \omega^2\psi \quad (1)$$

The potential

$$V(z) = \frac{1}{\sqrt{\rho c_s/r^2}} \frac{d^2}{dz^2} \sqrt{\rho c_s/r^2} - \frac{4Gm}{r^3} \quad (2)$$

incorporates thus the spatial variations of density  $\rho$ , sound speed  $c_s$  and spherical effects, as well as gravity. This problem is very similar to that encountered in the study of wind instruments, such as the trumpet, where Eq. 1 is known as the Bernoulli-Webster equation.

In Cepheids and RR Lyrae the hydrogen partial ionization, in which  $c_s$  varies extremely rapidly, produces a very sharp and enormously high potential barrier, that splits the pulsating envelope into two almost disjoint parts (*cf.* Paper I). Using the scaled eigenvectors  $\Psi$  one readily sees that the 'normal' vibrational modes have a large amplitude

in the interior region. It is however also possible for some modes to be predominantly trapped in the outer region – these surface modes are the 'strange' modes.

When, as is customary, the modes are classified with increasing number of nodes (and thus increasing frequency) the strange modes appear when a quarter wavelength fits approximately into the surface region. For a typical  $5M_{\odot}$  Cepheid on the left of the instability strip one finds that the strange modes have  $n = 10 - 12$ , and somewhat smaller  $n$  on the cold side of the instability strip because there is more matter outside the partial ionization region of H.

When nonadiabatic effects, which are weak in Cepheids, are properly taken into account, the modal frequencies acquire of course an imaginary component. Most of the stellar envelope is damping, but the partial ionization zones cause strong pulsational driving. Since the strange mode has at best a very small amplitude in the He partial ionization region it thus experiences no driving or damping there. All its driving must occur in the H partial ionization region. It is not possible to extend the simplified description of driving found in textbooks (*e.g.*, Cox & Giuli 1965) to modes higher than the fundamental or the first overtone. For the higher modes the driving or damping are a delicate function of the relative phase of the pressure and specific volume eigenfunctions which exhibit an increasing number of oscillations (related to the nodes in the adiabatic limit) (*e.g.*, Glasner & Buchler 1993, Buchler, Yecko, Kolláth 1997) as the work-integral shows

$$W_k = \frac{2\pi}{I_k} \text{Im} \int \delta p_k^* \delta v_k dm \quad (3)$$

$$= -\frac{2\pi}{I_k} \int |\delta p_k| |\delta v_k| \sin(\phi_v - \phi_p)_k dm \quad (4)$$

$$I_k = \omega_k^2 \int |\delta r_k|^2 dm \quad (5)$$

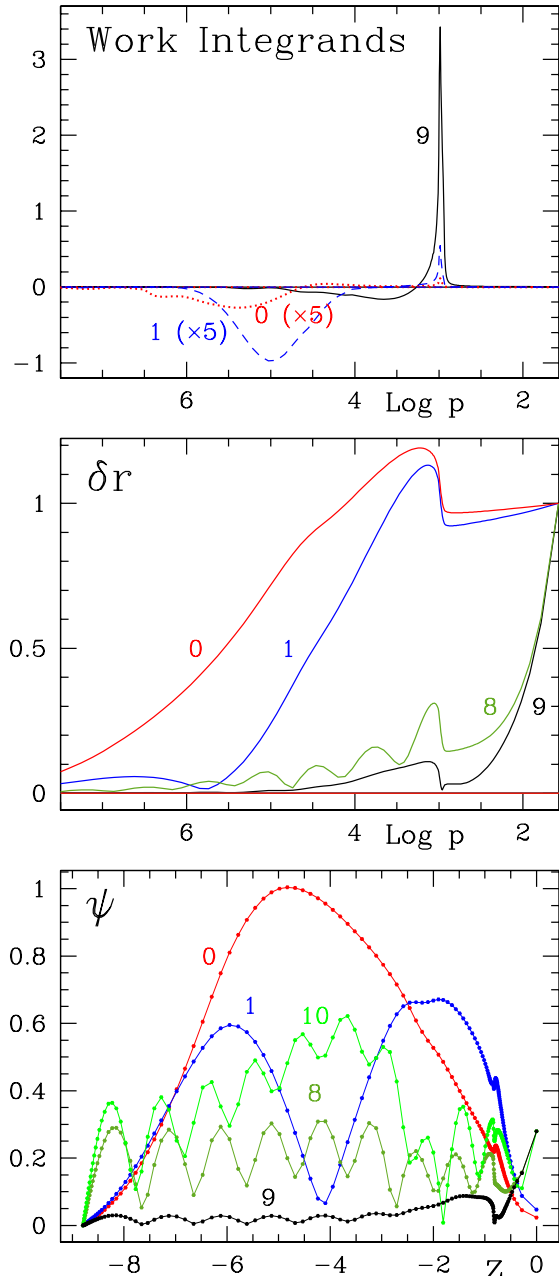


Fig. 1. – Cepheid model,  $M=8$ ,  $L=10000$ ,  $T_{\text{eff}}=6700$  K model; *Top*: work-integrand *w vs.*  $\text{Log}_{10}(\text{pressure})$  [cgs] for modes 0 (fundamental), 1 (first overtone) and 9 (strange mode); *middle*: radial displacement eigenvectors for modes 0, 1, 8 and 9; *bottom*: transformed radial displacement eigenvector ( $\Psi$ ) as a function of acoustic depth  $z$  (for clarity mode 1 has been scaled up by a factor of 2 and modes 8–10 by 12).

In Fig. 1 (middle) we exhibit the linear displacement eigenvectors (modulus) as a function of  $\text{Log } p$  of the fundamental, first overtone and strange 9th overtone for a Cepheid model with  $M=8M_{\odot}$ ,  $L=10000L_{\odot}$ ,  $T_{\text{eff}}=6700$  K,  $X=0.70$ ,  $Z=0.02$ . Clearly that the strange mode is very strongly restricted to the surface region.

This even more apparent in the bottom of Fig. 1 which displays the scaled displacement eigenvectors  $\psi$  (*cf.* Eq. 1)

as a function of acoustical depth  $z$  for the fundamental, first overtone, and for overtones 8 through 10. As pointed out in Paper I, this representation of the modes as  $\psi(z)$  brings out the vibrating string nature of the modes, and shows that the strange mode (9th overtone) is mainly a surface mode in contrast to its neighbors.

In the top Fig. 1 which displays the work-integrand as a function of  $\text{Log } p$ , the integrand is normalized so that the area under the curve represents the relative growth-rate  $\eta = 2\kappa_k P_k$ . The solid line represents the strange mode (9th overtone). For comparison we also show the work-integrands (multiplied by 5 for improved visibility) for the fundamental (dotted) and first overtone (dashed). The latter modes are very stable for this model which is on the left of the instability strip (*cf.* Fig. 1). The strange mode is restricted to the surface regions and its driving comes entirely from the H partial ionization region around  $\text{Log } p \sim 3$ .

Some simple *a posteriori* explanation of the odd stability properties of the strange modes can be given. The strange modes penetrate much less deeply than the normal modes. For the strange modes  $W_k$  is thus (a) totally dominated by the outer regions, in particular the hydrogen partial ionization region, and (b)  $W_k$  is much smaller. However, its the moment of inertia  $I_k$  is also very small because the mode is localized in the surface. Since the smaller work-integrals  $W_k$  are normalized by the smaller  $I_k$ , the strange modes still have relative growth-rates that are comparable in magnitude to those of the normal modes. However, because only hydrogen driving contributes, the growth-rates of the strange modes are egregious as was already shown in Paper I. In that paper strange modes were found to be vibrationally *unstable* to the left (blue) of the usual fundamental and first overtone instability strips.

Furthermore nonlinear hydrodynamical modelling indicated that the strange modes can give limit cycles, albeit with rather small pulsation amplitudes, typically in millimagnitudes. This has opened the exciting possibility of observing ‘strange Cepheids’, and of using such additional information to put constraints on theoretical Cepheid modelling.

Two questions were left unanswered in Paper I, however. The first concerned the surface boundary condition, namely the disregard of the surface impedance, due to the reaction of the isothermal atmosphere and of running wave or acoustic damping. The second resulted from the neglect of turbulence and convection which can also affect driving and damping. Here, in §2 we reexamine and improve on the outer boundary condition. In §3 and §4 we examine turbulent convective Cepheid and RR Lyrae models. In §5 we present nonlinear pulsations of turbulent convective models and we conclude in §6.

## 2. ISOTHERMAL ATMOSPHERE AND BOUNDARY CONDITIONS

In paper I the models were integrated up to a point where the gas pressure was small, typically a few times the radiation pressure. In the linearization of the discretized equations we imposed a standard condition of a zero Lagrangean pressure variation,  $\delta p_* = 0$ , *i.e.*, to an open and perfectly reflecting boundary. This boundary condition disregards two effects, first, running, escaping waves, and second, inertial effects due to the isothermal atmosphere.

In acoustic parlance, these effects give rise to resistive and reactive surface loads (Morse & Ingard 1968).

It is interesting to note that the change of variables from  $\delta r$  to  $\Psi$ , because of the density dependence, effectively changes the problem from an 'open quarter-wave length tube' to a 'closed half-wave length tube'. (Here we have taken the stellar surface to be defined as the point where the gas pressure equals two times the radiation pressure, *i.e.*, at a very low density.)

Another way of looking at this is to say that when  $\omega$  is sufficiently large, the concomitant wave length gets sufficiently short compared to the isothermal scale height  $1/\alpha$  so that reflection at the surface becomes incomplete and acoustic energy is lost into the atmosphere.

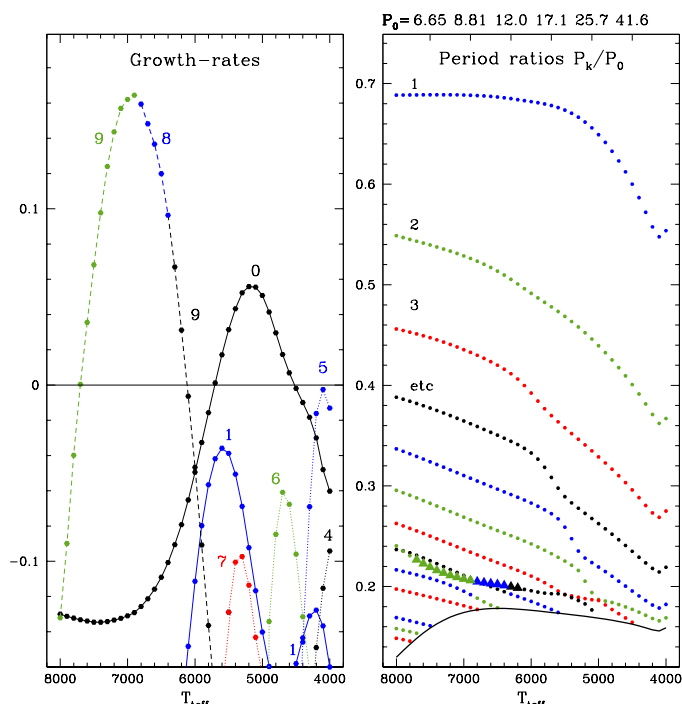


Fig. 2. – Cepheid model,  $M=8M_{\odot}$ ,  $L=10000L_{\odot}$ . *Left*: growth-rates as a function of  $T_{\text{eff}}$ , positive growth-rates correspond to linear unstable modes. The modes are labelled with the modal number. *Right*: period ratios  $P_k/P_0$  as a function of  $T_{\text{eff}}$ . The fundamental period  $P_0$  [d] is indicated on top. The triangles denote the unstable overtone modes. The solid line at the bottom is the isothermal cut-off period ratio.

In the optically thin outer region of the Cepheid model is essentially isothermal  $T \rightarrow (1/2)^{1/4} T_{\text{eff}}$ . To a good approximation the density decreases exponentially with scale height  $\alpha^{-1} = \mathcal{R}T/(\mu g)$ , where  $g = GM/r^2$  is essentially constant. This gives rise to a potential barrier which rapidly flattens to a constant value of  $V_* = (c_s \alpha/2)^2$ . In Buchler, Whiting & Kollath (2001) it is shown that the presence of the isothermal atmosphere can be approximately taken into account through a boundary condition that is imposed at the base of this atmosphere for the modes below the barrier ( $\omega < \omega_c$ ). The modes above the barrier disappear into the continuum and are no longer

astrophysically relevant.

$$\mathcal{S} \equiv (\Psi'/\Psi)_o = -ik \frac{(\omega + k) + (\omega - k) \exp(-2ik\Delta)}{(\omega + k) - (\omega - k) \exp(-2ik\Delta)} \quad (6)$$

where  $k \equiv k_r + ik_i = \sqrt{\omega^2 - V_*}$ . When  $|k_i \Delta|$  is large then  $\mathcal{S} \sim ik \text{sgn } k_i$ . The approximation that is inherent in the expression for the boundary condition is that the potential is a square barrier of width  $\Delta$ . This translates into a boundary condition

$$\delta p_* = \Gamma_1 p_* \left( -1 + (-\alpha/2 + \mathcal{S}) R_* \right) \delta r / R_* \quad (7)$$

With this new boundary condition our eigenvalue problem becomes more complicated and delicate. We compute the eigenvalues with a modified Castor method in which the  $\delta p_*$  of Eq. 7 replaces the usual  $\delta p_* = 0$  boundary condition. The presence of strange modes and their frequent proximity to the regular modes makes the Castor search difficult. We therefore first compute all the nonadiabatic eigenvalues for the  $\delta p_* = 0$  case with a general eigenvalue solver (*e.g.*, Glasner & Buchler 1993) and then switch on the new boundary condition gradually.

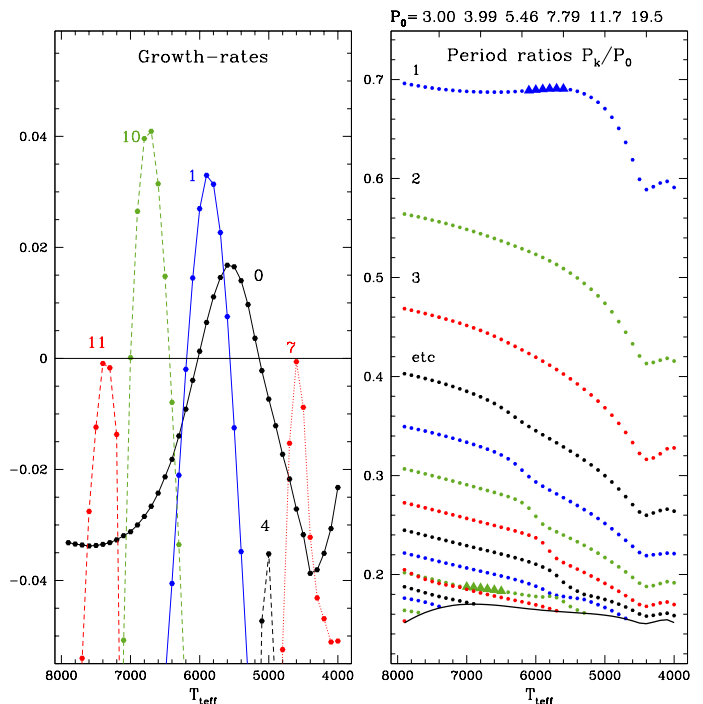


Fig. 3. – Cepheid model,  $M=6M_{\odot}$ ,  $L=3000L_{\odot}$ ; *cf.* Fig. 2 for legend.

### 3. TURBULENT CONVECTIVE CEPHEID MODELS

Turbulent convection changes the structure of the outer envelope, as well as the pulsational driving. To study its effects on the strange modes and to ascertain that they survive convection, we have used the Florida code (Yecko, Kolláth & Buchler 1998) with the  $\alpha$ 's defined as in Feuchtinger, Buchler & Kollath (2000) with values that are very similar to those used in our study of first overtone Cepheids, *viz.*  $\alpha_d = 2.177$ ,  $\alpha_c = 0.4$ ,  $\alpha_s = 0.433$ ,  $\alpha_\nu = 0.12$ ,  $\alpha_t = 0.001$ ,  $\alpha_r = 0.4$ ,  $\alpha_p = 0$  and  $\alpha_l = 1.5$ . We use the OPAL opacities of Iglesias & Rogers (1996) and of Alexander & Ferguson (1994).

In Figs. 2, 3 and 4 we show the results for 3 sequences of Cepheid models of fixed mass and luminosity over a broad range of  $T_{\text{eff}}$ . The left subfigures show the growth-rates as a function of the  $T_{\text{eff}}$  of the equilibrium models. The growth-rates for the unstable modes are positive. Some modes are very stable and lie below the graph.

As a function of  $T_{\text{eff}}$  the modal number (ordering with period) of the strange mode changes since it switches its properties with the regular modes through avoided crossings (*cf.* Paper I). It is therefore ambiguous how we should label the modes along a sequence, but this labelling is not important for us since we are interested in finding out whether there is an unstable strange mode and what its period is, both of which are unambiguous.

The instability strip of the  $8M_{\odot}$  in Fig. 2 extends from the fundamental blue edge at  $T_{\text{eff}}=5700$  K to the fundamental red edge at  $T_{\text{eff}}=4600$  K. An unstable strange mode exists from 7700 K through 6100 K which is the 11th overtone at the lower  $T_{\text{eff}}$ , but which gradually morphs into the 8th overtone by the time it gets to 8000 K. A correspondingly erratic behavior shows up in the period ratios. It is not a numerical artifact, but arises from avoided level crossings (*cf.* Paper I) that are also familiar from the quantum mechanical behavior of an atom in a B field and from the nonradial  $p + g$  spectrum in unevolved stars.

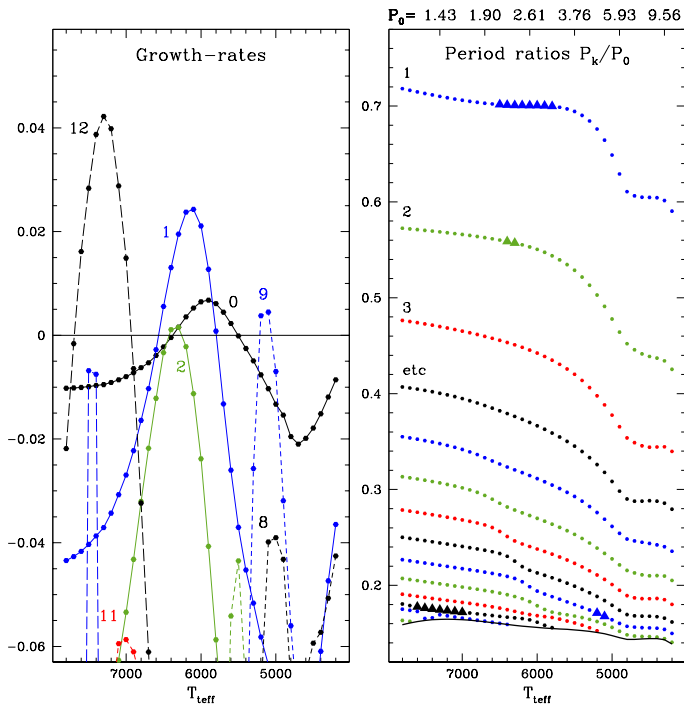


Fig. 4. – Cepheid model,  $M=4M_{\odot}$ ,  $L=860L_{\odot}$ ; *cf.* Fig. 2 for legend.

The instability strip of the  $6M_{\odot}$  model in Fig. 3 extends from the first overtone blue edge at  $T_{\text{eff}}=6200$  K to the fundamental red edge at  $T_{\text{eff}}=5150$  K. From 7000 K to 6450 K the 10th overtone is unstable. Around 5000 K the 8th overtone just misses being unstable.

The instability strip of the  $4M_{\odot}$  model Fig. 4 extends from the first overtone blue edge at  $T_{\text{eff}}=6550$  K to the fundamental red edge at  $T_{\text{eff}}=5500$  K, and it includes a small region with second overtone instability. From 7700 K to

6950 K the 12th overtone is unstable, and from 5200 K to 5100 K it is the 9th overtone.

#### 4. TURBULENT CONVECTIVE RR LYRAE MODELS

We consider an RR Lyrae model with  $M=0.65M_{\odot}$ ,  $L=45L_{\odot}$  with  $X=0.70$ ,  $Z=0.02$ . Fig. 5 shows that the instability strip of the model extends from the first overtone blue edge at  $T_{\text{eff}}=7250$  K to the fundamental red edge at  $T_{\text{eff}}=6000$  K. From 8300 K to 7200 K the 10th overtone is unstable, and from 5900 K to 5800 K the 8th overtone is unstable.

Again, these results show that an excited strange mode can exist on either side of the classical instability strip.

#### 5. NONLINEAR BEHAVIOR

The full amplitude pulsations have been computed with the Florida hydrodynamics code (Kolláth, Beaulieu, Buchler & Yecko, 1998) with the same mesh and parameters as used for the linear properties. The pseudo-viscosity was taken to be zero in our calculations.

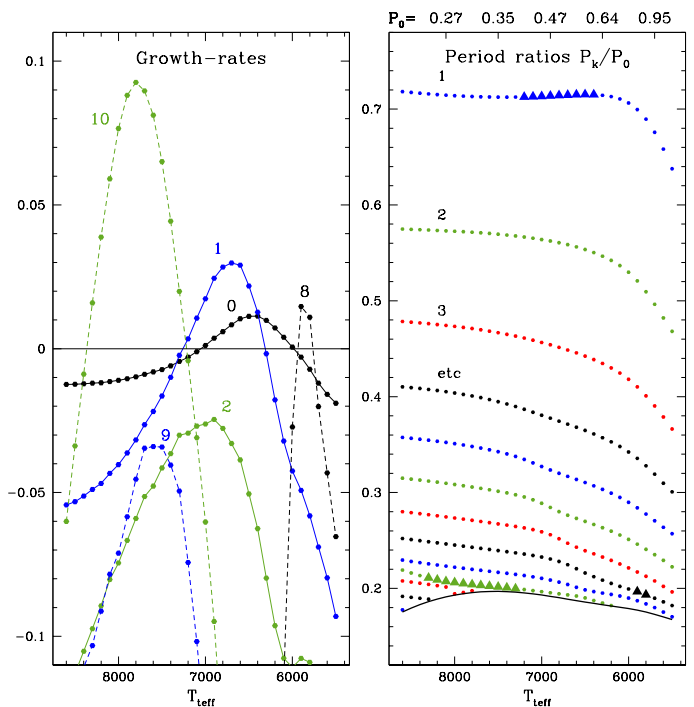


Fig. 5. – RR Lyrae model,  $M=0.65M_{\odot}$ ,  $L=45L_{\odot}$ ; *cf.* Fig. 2 for legend.

In Fig. 6 we exhibit the light and radial velocity curves for three selected Cepheid models and on RR Lyrae model. The lightcurves are measured in millimag, and the radial velocities in units of 100 m/s. Note that five of the models (1, 3 – 6) are blue strange variables, *i.e.*, they lie to left of the blue edge, and two (2 and 7) are red strange variables, *i.e.*, they lie to right of the blue edge. Interestingly they all have about the same pulsation amplitudes. Because the oscillation amplitude is so small and it is so confined to the surface region, there is not much matter below the photosphere that can modulate the heat flow. The light-curve amplitudes are therefore also small, in the millimagitude regime, but they are observable.

The temporal structure of the photospheric velocities

appears strange at first. In Fig. 7 we therefore show the behavior of the velocities throughout most of the model, in fact Lagrangean zones 65 through 145 of a 150 mass-shell model. The interior zones are essentially quiescent because of the high modal number of this mode. On the other hand the amplitude of the very outer zones increases considerably (but is not relevant because it contains so little mass and is considerably above the photosphere. The photosphere itself, which is shown as a single dashed line, is relatively quiescent. For reference we also show the hydrogen partial ionization region with three adjacent dashed lines. The helium ionization lies below in zones that are not shown because the velocities are small. The photosphere is seen to lie in a relatively quiescent region and is subjected to inward and outwards moving ripples that account for its sometimes strange looking behavior in Fig. 6.

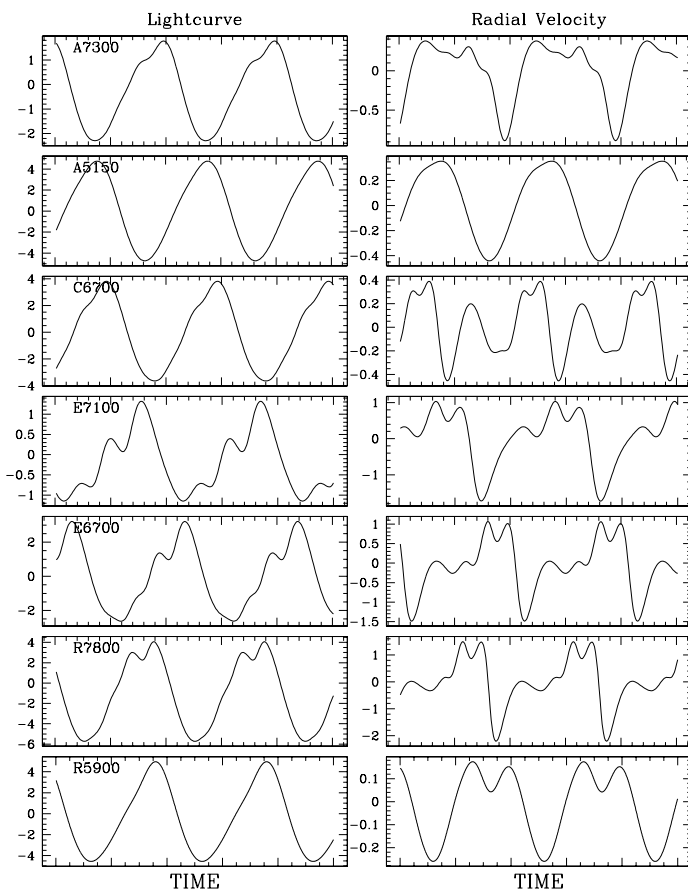


Fig. 6. – *Left*: Light curves (in millimag): *Right*: radial velocity curves (in 100m/s). From top to bottom, Cepheids:  $M=4M_{\odot}$  [A],  $T_{\text{eff}}=7300$  and  $5150$  K,  $M=6M_{\odot}$  [C],  $T_{\text{eff}}=6700$  K,  $M=8$  [E],  $T_{\text{eff}}=7100$  and  $6700$  K, RR Lyrae:  $M=0.65M_{\odot}$  [R],  $T_{\text{eff}}=7800$  and  $5900$  K.

There are two shortcomings to these calculations. First, the (linear) special boundary condition at the outer surface (Eq. 7) has not been incorporated in the nonlinear code, but we do not expect that to cause a major distortion, for the pressure is so small at the boundary. Second, what is perhaps more severe, there is no provision for acoustic leakage in the nonlinear hydrodynamics code for waves

with frequencies above the isothermal threshold  $\omega_c$ .

The presence of higher frequency reflected waves is perhaps the reason for the pronounced harmonic wiggles on the light curves and especially in the radial velocity curves. Indeed, because spherical effects are negligible, the higher order strange modes are all in resonance. However, if they are excited along with the lowest strange mode, then the even harmonics should be absent, but they are not.

## 6. DISCUSSION AND CONCLUSION

The improved boundary conditions have a small effect on the behavior of the deep modes, mostly because the pressure variation at the stellar surface  $\delta p_*$  is always small. However, they do affect the higher overtones as they approach the cutoff frequency by shifting their periods, sometimes causing inversions in the modal ordering and affecting the stability of the modes.

Turbulent convection does not kill the linear instability of the strange modes, as one might have feared. On the contrary, they are as unstable as with the radiative models. One even finds unstable strange modes to the right of the fundamental red edge.

The growth-rates of the strange modes on the hot side of the instability strip are not very sensitive to turbulent convection. On the other hand convection is very strong in the cooler models, and the values of the stability coefficients of the strange modes on the cool side are consequently less certain than they are on the hot side.

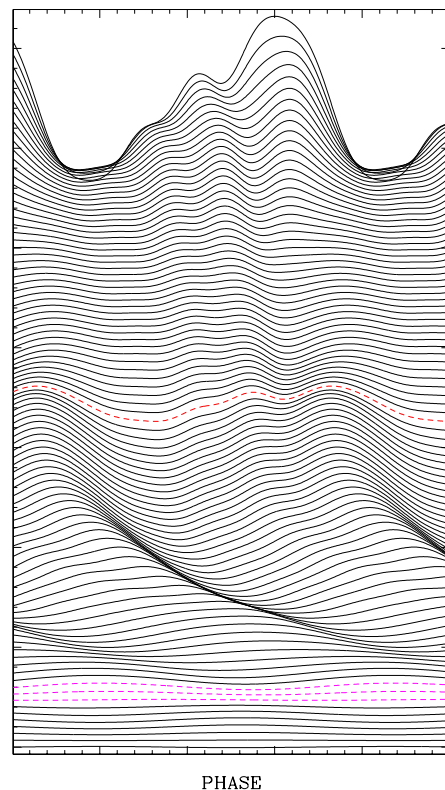


Fig. 7. – Radial velocity profile for the Cepheid model  $M=6M_{\odot}$ ,  $T_{\text{eff}}=6700$  K; the individual Lagrangean zones (zones 65 through 145 for a 150 zone model) are shifted vertically for better visualization; the dashed line corresponds to the photospheric velocity. the three adjacent dashed lines denote the hydrogen partial ionization region

So, do strange Cepheids really exist in nature? We find the occurrence of self-excited strange modes to be quite robust, *i.e.*, largely independent of any modelling parameters. For an individual model the change in modelling parameters may have a large effect, but when one considers a whole sequence of models one finds that modelling parameters (*e.g.*, the fineness of the grid) merely cause a small shift (*e.g.*, in  $T_{\text{eff}}$ ). Especially in the high luminosity Cepheid models, the strange mode has a period well above the isothermal cutoff period as the right hand side of Fig. 2 shows. For the low mass Cepheids and the RR Lyrae some of the unstable strange modes occur very close to the isothermal cutoff frequency  $\omega_c$ . This cutoff frequency however is somewhat uncertain because it depends on the structure of the dilute atmosphere which itself is sensitive to the treatment of radiative transport (treated here in the customary diffusion approximation).

We find furthermore that the full amplitude (nonlinear) pulsations are quite robust in all cases. However, the values of the pulsation amplitudes are somewhat un-

certain because they depend on modelling parameters as they did for the classical Cepheid pulsations. In particular the turbulent eddy viscosity has a large effect. (We recall that our convective parameters  $\alpha$ 's were calibrated to give good agreement with the observations of classical Cepheids, Feuchtinger *et al.* 2000).

The detection of this type of pulsation would be very important because it would add very strong additional constraints on the Cepheid and RR Lyrae modelling. The search for millimagnitude variability on either side of the classical instability strip with periods approximately 1/4 to 1/5th the fundamental period (*cf.* Figs. 1–3, 5) would be required. Hopefully this will become possible with COROT.

## 7. ACKNOWLEDGEMENTS

It is a pleasure to thank Phil Yecko and Bernard Whiting for fruitful discussions. This work has been supported by NSF (AST 98-19608).

## REFERENCES

- Alexander, D. R., Ferguson, J. W. 1994, ApJ 437, 879  
 Buchler, J. R., P. Yecko & Kolláth, Z 1997, A&A 336, 553  
 Buchler, J. R., Whiting, B. & Kolláth, Z 2000, A&A, in preparation  
 Cox, J. P. & Giuli R. T. 1969, *Principles of Stellar Structure* (New York: Gordon and Breach)  
 Feuchtinger, M., Buchler, J. R. & Kollath, Z., 2000, *Hydrodynamical Survey of First Overtone Cepheids*, ApJ (in press),  
 Gautschy, A. & H. Saio, 1995, Ann. Rev. Astr. Astrophys 33, 75 and 1996, *ibid.* 34, 551  
 Glasner, A. & Buchler, J.R. 1993, A&A 277, 69.  
 Iglesias, C.A. & Rogers, F. J., 1996, ApJ 464, 943  
 Kolláth, Z., Beaulieu, J.P., Buchler, J. R. & Yecko, P., 1998, *Nonlinear Beat Cepheid Models*, ApJ Lett 502, L55  
 Kolláth, Z. & Buchler, J. R., 2000, in *Nonlinear Studies of Stellar Pulsation*, Eds. M. Takeuti & D.D. Sasselov, ASS Lib Ser (in press), [<http://xxx.lanl.gov/abs/astro-ph/0003386>]  
 Kolláth, Z., Buchler, J. R. & Yecko, P. 1997, ASS Libr. Ser., Eds. M. Takeuti & D. Sasselov (in press)  
 Morse, P. M. & Ingard, K. U. 1968, *Theoretical Acoustics*, (New York: McGraw Hill)  
 Saio, H., Wheeler, C.J. & Cox, J.P. 1984, ApJ 281, 318  
 Yecko, P., Kolláth, Z. & Buchler, J. R. 1998, AA 336, 553